CD20 as target for immunotherapy

Engelberts, P.J.

3

A quantitative flow cytometric assay for determining binding characteristics of chimeric, humanized and human antibodies in whole blood: proof of principle with rituximab and ofatumumab

J Immunol Methods. 2013 Feb 28;388(1-2):8-17.

- Patrick J. Engelberts[1*], Carole Badoil[2*], Frank J. Beurskens[1], Danièle Boulay-Moine[2], Karine Grivel[2], Paul W.H.I. Parren[1], Maxime Moulard[2].

1 Genmab, Utrecht, The Netherlands.

2 BioCytex, Marseille, France.

* Both authors contributed equally

ABSTRACT

Clinical successes of antibody-based drugs has led to extensive (pre-) clinical development of human(ized) monoclonal antibodies in a great number of diseases. The high specificity of targeted therapy with antibodies makes it ideally suited for personalized medicine approaches in which treatments needs are tailored to individual patients. One aspect of patient stratification pertains to the accurate determination of target occupancy and target expression to determine individual pharmacodynamic properties as well as the therapeutic window. The availability of reliable tools to measure target occupancy and expression on diseased and normal cells is therefore essential. Here, we evaluate a novel human antibody detection assay (Human-IgG Calibrator assay), which allows the flow cytometric quantification of therapeutic antibodies bound to the surface of cells circulating in whole blood. This assay not only permits the determination of the number of specific antibody binding capacity (sABC), but, when combined with quantification of exogenously added mouse antibody, also provides information on binding kinetics and antigen modulation. Our data indicate that the calibrator assay has all properties required for a pharmacodynamic tool to quantify target occupancy of chimeric, humanized and human therapeutic antibodies during therapy, as well as to collect valuable information on both antibody and antigen kinetics.

INTRODUCTION

In antibody based therapy, efficient antibody binding kinetics and sufficient target occupancy are critical for achieving and maintaining clinical efficacy. Monitoring these parameters in a standardized manner, can be employed to evaluate and tailor therapeutic regimes to achieve maximal effects for individual patients in personalized medicine approaches. Measuring both antigen surface expression and therapeutic antibody target occupancy on malignant and normal cells, thus provides valuable information on: 1. Target occupancy, which can be predictive for the optimal use of desired antibody-mediated effector functions [1-4]; 2. Antigen surface expression, which can serve as a diagnostic tool [5-10]; and 3. Antigen modulation during therapy, which can be indicative for durable therapeutic efficacy [11-18].

A widely accepted approach to quantify antibodies bound to cells or cell surface proteins is the use of quantitative flow cytometry (QFCM), which allows quantification of the number of molecules of a defined antigen expressed on the surface of cells. Two QFCM methods can be distinguished into direct and indirect immunofluorescence. Direct QFCM makes use of a fluorochrome-conjugated primary antibody, whereas indirect QFCM makes use of a fluorochrome-conjugated secondary antibody to detect and quantify the primary antibody bound. Both QFCM methods employ the use of calibration beads to convert fluorescence intensity of a sample into a value corresponding to the number of antibody molecules bound, either in Molecules of Equivalent Soluble Fluorochromes (MESF)

or specific Antibody Bound per Cell (sABC) [19-21]. As the direct fluorescence approach requires conjugation of primary antibodies for the conversion of MFI to MESF or sABC, this method can only be used in *in vitro* or *ex vivo* settings. For the indirect fluorescence approach no pre-conjugation of the antibody to be detected is required, and hence can be employed to study the therapeutic agent in real time during the course of the treatment.

The field of QFCM measurement has taken a huge leap over recent years; on the one hand due to the enforcement of regulations and standards set by regulatory authorities, on the other hand owing to the increased commercial availability of standardized kits and reagents [22,23]. Various studies have reported on the validity [5], accuracy [24] and inter-laboratory variations [25] of QFCM. Here we explore the potential of incorporating QFCM into the clinical setting, where it is used to determine maximum and actual target occupancy by a therapeutic antibody on cells in patient-derived material, such as whole blood or bone marrow. We have studied these characteristics for the human IgG calibrator assay. This newly developed quantitative indirect fluorescence immunoassay can detect and enumerate antibodies that contain human constant domains including chimeric, humanized and fully human antibodies, bound to target cells. The clinically validated target CD20 (a B-cell specific membrane tetra-spanning protein) is used to examine target occupancy on normal and malignant B-cell lines by two FDA/EMA approved monoclonal antibody (mAb) products: rituximab (RTX), a chimeric IgG1 mAb [26] and ofatumumab (OFA), a human IgG1 mAb [27].

MATERIAL AND METHODS

Blood samples and cell lines

Peripheral whole blood (WB) from healthy donors was drawn, with informed consent, into sterile lithium heparin or K3-EDTA tubes.

The Burkitt lymphoma cell lines Raji and Ramos were obtained from American Type Culture Collection (ATCC) and Daudi from Deutsche Sammlung von Mikroorganismen und Zellkulturen (DSMZ). Cells were grown as suspension cultures in RPMI-1640 medium supplemented with 10% heat-inactivated fetal calf serum, 2 mM L-glutamine, 1 mM sodium pyruvate, 50 U/mL penicillin and 50 µg/mL streptomycin. The human chronic B-cells leukaemia cell line MEC-1 was obtained from DSMZ. The culture medium for MEC-1 was IMDM, supplemented with 10% heat-inactivated fetal bovine serum, 2 mM L-glutamine, 1 mM sodium pyruvate, 50 U/mL penicillin and 50 µg/mL streptomycin.

Cells were propagated at 37°C with 5% CO_2 in a humidified incubator.

Antibodies

The primary mAbs used are detailed in Table 1.

The secondary antibodies mouse-IgG absorbed goat anti-human IgG FITC (BioCytex) and human-IgG absorbed goat anti-mouse IgG FITC (BioCytex) were used as conjugates for the human IgG calibrator assay and the mouse IgG calibrator assay, respectively. The pre-absorption on mouse IgG of anti-human IgG and on human IgG of anti-mouse IgG removes all potential cross-reactivity between the two species.

TABLE 1 mAbs used in this study.

mAb	Target	Isotype	Form	Source
rituximab (RTX)	CD20	Chimeric IgG1	Purified	Roche
ofatumumab (OFA)	CD20	Human IgG1	Purified	Genmab
HuIgG1-7D8	CD20	Human IgG1	Purified	Genmab
MuIgG1-7D8	CD20	Mouse IgG1	Purified	Genmab
MuIgG2a-7D8	CD20	Mouse IgG2a	Purified	Genmab
Clone B9E9	CD20	Mouse IgG2a	Purified	Beckman Coulter
Clone 4H10	KLH	Mouse IgG2a	Purified	BioCytex
Clone 2H11/2H12	DNP	Mouse IgG1	Purified	BioCytex
Clone J4.119	CD19	Mouse IgG1	Purified, PC5-conjugated	Beckman Coulter

Immunostaining

Before immunostaining, red blood cells (RBC) from WB samples were lysed (lysis solution from BioCytex) for 10 min at 4°C and washed in wash buffer (PBS – 0.1% BSA – 0.09% sodium azide; BioCytex). When notified, lysis step was performed after immunostaining step.

All immunostaining incubation steps, unless otherwise indicated, were performed for 10 min at 4°C. After each incubation step, samples were washed with wash buffer.

For the determination of antibody binding sites, samples (white blood cells from WB or cell lines) were incubated with either a concentration range of primary anti-CD20 antibody, to determine the amount of bound antibodies at specific primary antibody concentrations, or with a saturating concentration of primary antibody (30 µg/mL) to determine the density of antigen.

An optional acidic wash with cold acetic acidic solution (0.5M NaCl, 0.2M acetic acid, pH=2.6) for 2 min at 4°C was included after the primary antibody incubation, to determine baseline expression. Efficacy of acidic wash and reprobing were tested by adding an incubation step of respectively buffer or saturating concentrations of primary antibody (30 µg/mL).

To assess the CD20 occupancy, samples were first incubated with a concentration range of primary antibody, and washed. When specified, an acidic wash was performed. Subsequently, by adding saturating amounts (30 µg/mL) of primary antibody or buffer, the levels of maximum of binding capacity (Max ABC; sample with additional saturating amount of primary antibody) and bound primary antibody (Bound sABC; sample with buffer addition) can be determined. Background and baseline expression were determined using the acid wash step.

For the dissociation and internalization measurements, saturating amounts of primary human antibody were incubated with the samples for 10 min at 37°C. After washing with wash buffer, a 100 fold-excess amount of mouse antibody was added to prevent human primary antibody rebind-

ing and samples were measured at different time points.

After binding of the primary antibody, samples were washed in wash buffer and mAbs bound to the surface were stained for 10 min on ice with FITC-labelled goat anti-human IgG (BioCytex) or FITC–labelled goat anti-mouse IgG (BioCytex). In parallel, calibration beads were also treated with FITC-labelled goat anti-human IgG or FITC–labelled goat anti-mouse IgG for 10 min on ice. Samples and beads were washed. An additional step of counterstaining was run for WB samples. Anti CD19-PC5-coupled mAb was added to samples from WB to identify B-cells. After 10 min at 4°C incubation, WB samples were washed. Samples and beads were fixed overnight at 4°C with a 1% paraformaldehyde solution and analyzed by flow cytometry using FC500 or Gallios cytometers (Beckman Coulter).

Sample analysis

For analysis of number of antibody binding sites (Figure 1), cell fragments and RBC ghosts were removed by gating total leukocytes or cell lines on a FSC/SSC plot. B-cells from WB samples were isolated from total leukocytes by gating on a CD19-PC5/SSC plot. Gated cell lines or B-cells were then displayed on a FL-1 histogram plot and an interval cursor was set to cover the main peak of FITC signal.
For the calibration beads, the MFI for each bead population was determined by application of separate interval cursors (M1, M2 and M3) and plotted against the number of antibodies coated on the beads (a predefined amount of an unrelated antibody coated on the surface which was standardized using radio immunoassays relative to ^{125}I-coupled IgG [data not shown]) allowing to draw a calibration curve.
The MFI from cells is reported in the calibration curve obtained from the beads, giving the ABC for the samples.

Calculations

Specific antibody binding sites (sABC) was calculated by subtracting buffer or isotypic negative control (anti-DNP or anti-KLH mAbs) ABC from CD20 mAb of interest ABC value.

FIGURE 1 The human IgG calibrator assay and the mouse IgG calibrator assay are based on the same quantification of indirect fluorescence immunoassay principle.
Both assays quantify the number of antibodies bound to the target by correlating the fluorescence intensity with that of a calibration curve.
In this study, CD20 is used as a target antigen. For the mouse IgG calibrator assay (**A.** right panel), the primary antibody is an antibody which is detected by a secondary FITC-labelled goat antibody against mouse IgG. For the human IgG calibrator assay (**A.** left panel), the primary antibody is a chimeric [RTX], humanized or human mAb [OFA]) and the secondary antibody is a FITC-labelled goat antibody against human IgG.
The primary antibody is allowed to bind to cells, after which cells and calibration beads (containing a known density of antibody) are labelled, in parallel, with a fluorescein-conjugated secondary antibody. The MFI obtained for the beads coated with a low amount (M1), an intermediate amount (M2) or high amount of antibody (M3) is then plotted against the actual amount of antibody molecules present on the beads. This provides a calibration curve that shows a linear correlation between antibody molecule numbers and fluorescence signal. The fluorescence signal obtained for each sample can then be converted to number of antibodies binding capacity (ABC) by interpolation in the calibration curve.

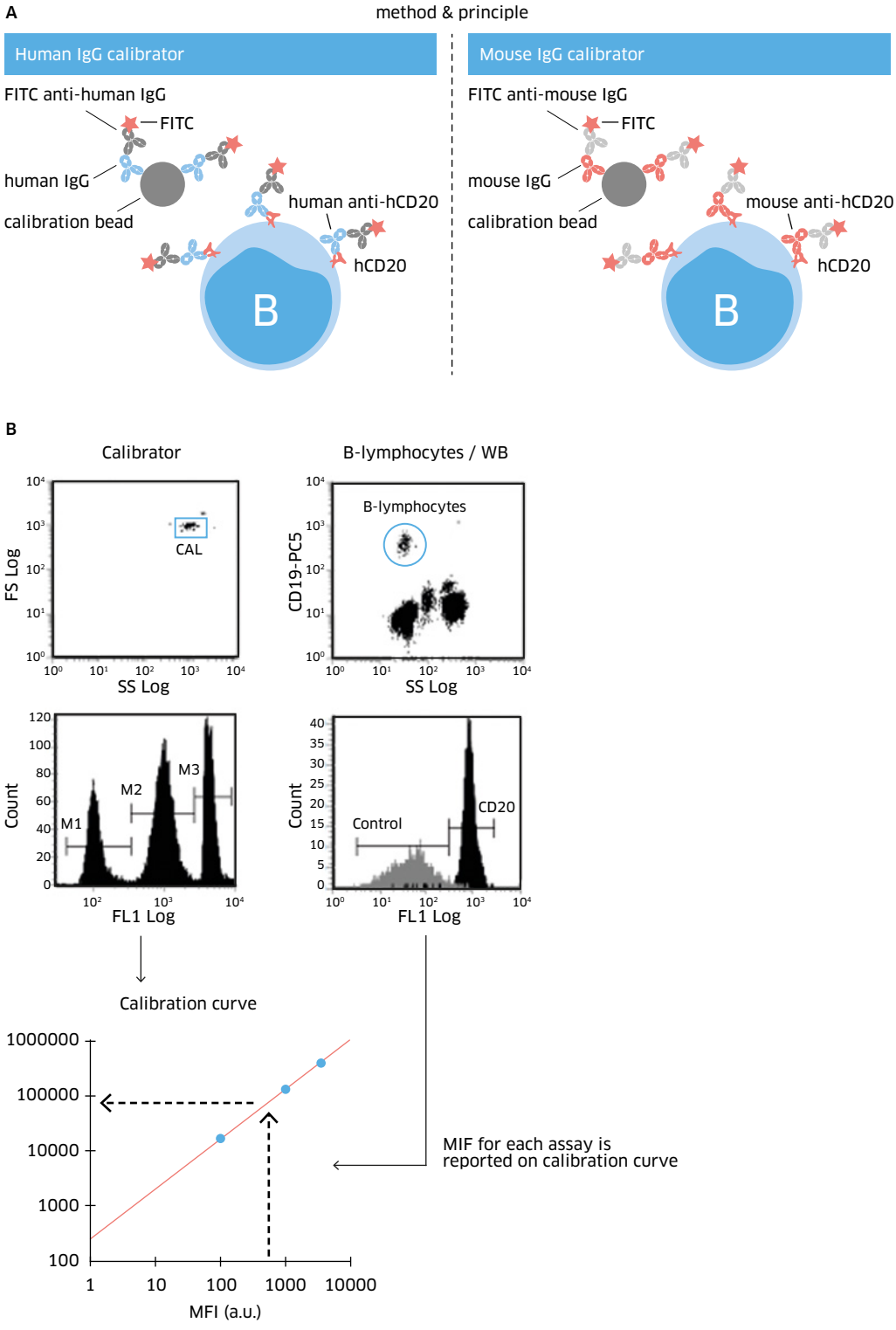
A
method & principle
Human IgG calibrator
FITC anti-human IgG
FITC
human IgG
calibration bead
human anti-hCD20
hCD20
B
Mouse IgG calibrator
FITC anti-mouse IgG
FITC
mouse IgG
calibration bead
mouse anti-hCD20
hCD20
B
B
Calibrator
B-lymphocytes / WB
FS Log
CAL
SS Log
CD19-PC5
B-lymphocytes
SS Log
Count
M1
M2
M3
FL1 Log
Count
Control
CD20
FL1 Log
Calibration curve
MIF for each assay is
reported on calibration curve
MFI (a.u.)

The apparent binding affinity constant K_d of the therapeutic CD20 mAbs was determined with Sigma Plot software (Systat Software, INC., San Jose, CA, USA) from the antibody concentration plot as determined with the human or mouse IgG calibrator assay with the following formula:

$$y = \frac{B_{max} \times \chi}{K_d + \chi}$$

Where y is the sABC, x is the primary mAb concentration, B_{max} is the maximal specific binding observed and K_d is the ligand affinity constant.

To determine the amount of occupied antibody binding sites opposed to the expressed amount of antibody binding sites, an extra incubation step was included with either buffer (Bound ABC converted in Bound sABC) or a saturating amount or primary antibody (Max ABC converted in Max sABC). Percentage of CD20 occupancy was calculated using the following formula:

$$\% \text{ occupancy} = \frac{\text{Bound sABC}}{\text{Max sABC}} \times 100$$

EC50 and EC90 values were determined from the occupancy experiment with Sigma Plot software using a 4-parameter logistic regression and using the following formula:

$$y = \min + \frac{\max - \min}{1 + 10^{(\log EC50 - \chi) \times \text{hillslope}}}$$

Where y is the observed response (% occupancy), x is the log of the mAb concentration, min and max are respectively the minimal and maximal observed values.

To study antibody and antigen kinetics the occupancy of bound human and mouse antibodies relative to the occupancy at the start of the experiment (time = 0) was determined according to formula described below:

$$\% \text{ binding (time = t)} = \frac{\text{sABC (time = t)}}{\text{sABC (time = 0)}} \times 100$$

The detection half-life $t_{1/2}$ and off rate k_{off} were determined from the graph log (sABC) plotted against time using Sigma Plot software.

statistical analysis

To determine the significance of differences in maximum sABC obtained for all mAbs on cell lines and WB samples, a one way analysis of variance was performed with a Tukey's multiple comparison tests as post-test. Results obtained using WB samples were subjected to repeated measures ANOVA (significant differences were defined by $P<0.05$).

RESULTS

Determination of Antibody Binding Sites

In a first set of experiments we studied the number of antibody molecules bound to cells by incubating Daudi cells with a concentration range of primary antibody (either human (Figure 2A) or mouse (data not shown)). Plotting the sABC to the antibody concentration resulted in an s-shaped binding curve. Saturation of binding sites was obtained at the highest primary antibody concentrations. From this plot we then determined both total

TABLE 2 Antibody binding sites

	Daudi		Raji		Ramos		MEC-1		B-Lymphocytes (from whole blood)	
	Mean (sABC)	SD (sABC)	Mean (sABC)	SD (sABC)	Mean (sABC)	SD (sABC)	Mean (sABC)	SD (sABC)	Mean (sABC)	SD (sABC)
Human calibrator										
ofatumumab	141.020	13.479	300.035	66.187	352.085	37.240	678.205	121.285	120.143	22.770
rituximab	119.207	18.896	259.729	66.983	325.314	42.013	621.247	112.605	129.629	32.276
h7D8	121.789	20.284	252.228	68.560	333.003	43.129	577.346	76.500	110.151	31.718
Mouse calibrator										
mIgG1-7D8	92.089	20.475	175.677	67.299	278.558	54.382	418.361	67.836	117.498	23.997
mIgG2a-7D8	100.353	20.494	210.281	78.549	280.335	71.952	490.789	58.568	132.425	29.095
B9E9	74.669	17.384	118.902	53.931	181.722	32.594	274.765	41.588	101.473	16.686

TABLE 3 Antibody kinetics

	Daudi		Raji		Ramos		MEC-1		Whole blood	
	EC_{50} (µg/mL)	SD (µg/mL)	EC_{50} (µg/mL)	SD (µg/mL)	EC_{50} (µg/mL)	SD (µg/mL)	EC_{50} (µg/mL)	SD (µg/mL)	EC_{50} (µg/mL)	SD (µg/mL)
Human calibrator										
ofatumumab	1,17	0,23	3,45	1,45	0,79	0,10	2,57	0,48	0,48	0,17
rituximab	1,61	0,14	5,61	1,70	1,87	0,53	4,11	0,41	0,81	0,51
h7D8	3,13	0,20	12,00	3,92	2,03	0,59	8,32	1,68	0,94	0,62
Mouse calibrator										
mIgG1-7D8	6,66	1,28	17,02	4,67	2,58	0,79	8,11	2,10	2,64	1,65
mIgG2a-7D8	6,88	1,01	13,74	3,50	2,80	0,49	7,08	1,06	1,98	1,69
B9E9	8,01	2,44	21,77	9,29	3,87	2,59	8,58	2,46	5,27	4,04

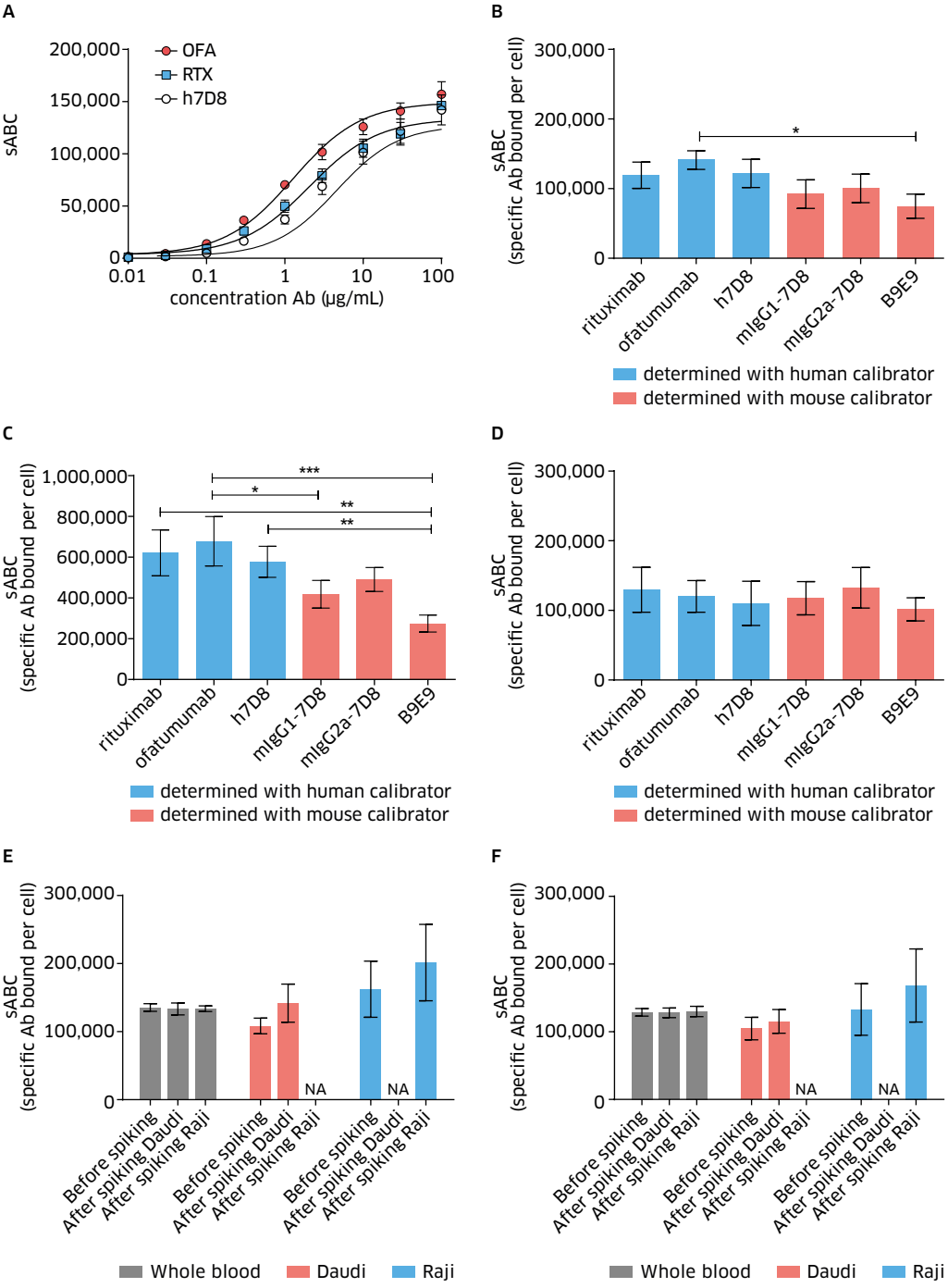
A
sABC
200,000
150,000
100,000
50,000
0
OFA
RTX
h7D8
0.01
0.1
1
10
100
concentration Ab (µg/mL)
B
sABC
(specific Ab bound per cell)
300,000
200,000
100,000
0
*
rituximab
ofatumumab
h7D8
mIgG1-7D8
mIgG2a-7D8
B9E9
determined with human calibrator
determined with mouse calibrator
C
sABC
(specific Ab bound per cell)
1,000,000
800,000
600,000
400,000
200,000
0
***
*
**
**
rituximab
ofatumumab
h7D8
mIgG1-7D8
mIgG2a-7D8
B9E9
determined with human calibrator
determined with mouse calibrator
D
sABC
(specific Ab bound per cell)
300,000
200,000
100,000
0
rituximab
ofatumumab
h7D8
mIgG1-7D8
mIgG2a-7D8
B9E9
determined with human calibrator
determined with mouse calibrator
E
sABC
(specific Ab bound per cell)
300,000
200,000
100,000
0
NA
NA
Before spiking
After spiking Daudi
After spiking Raji
Whole blood
Daudi
Raji
F
sABC
(specific Ab bound per cell)
300,000
200,000
100,000
0
NA
NA
Before spiking
After spiking Daudi
After spiking Raji
Whole blood
Daudi
Raji

FIGURE 2 The mouse and the human calibrator assays were used to enumerate the total number of antibodies binding capacity using a concentration curve of human CD20 mAbs and mouse mAbs.
In panel **A**, a representative binding curve of human antibodies (huIgG1-7D8, RTX and OFA) to Daudi cells is shown. By comparing the sABC obtained using saturating concentrations (30 μg/mL) of human mAbs (huIgG1-7D8, RTX and OFA) and mouse mAbs (muIgG1-7D8 and muIgG2a-7D8) both calibrator assay were compared on Daudi cells (**B**), MEC-1 cells (**C**) and B-lymphocytes from whole blood (**D**), (Bars represent an average of 3 measurements, error bars indicate SD). Statistical analysis indicate that the sABC obtained with OFA and RTX are not significantly different whereas RTX sABC and OFA sABC differed significantly (*, $p<0.05$; **, $p<0.01$; ***, $p<0.001$) from sABC for B9E9 (a probable type II CD20 mAb) on Daudi and MEC-1 cells but not on WB.
To show that the detection in sABC is not hampered by sample matrix such as whole blood, blood was mixed with Raji cells or Daudi cells and the amount of specific antibody binding capacity was determined with either the human (**E, in presence of huIgG1-7D8**) or mouse calibrator assay (**F, in presence of muIgG1-7D8**). Both for B lymphocytes and for Daudi and Raji cells the amount of sABC detected for muIgG1-7D8, muIgG2a-7D8 or huIgG1-7D8 at saturating concentration of antibody was similar in original samples and in the sample in which Raji cells were added to whole blood, indicating IgG in the sample matrix or on the surface of cells do not affect measurements.

bound antibody (in maximum sABC; at a saturating mAb concentration of 30 μg/mL) and $EC_{50,}$; results are shown in Table **2** and Table **3,** respectively. Similar to Daudi cells (Figure 2B), we also tested Raji (S1), Ramos (S2), MEC-1 (Figure 2C) cells and B lymphocytes from WB (Figure 2D) for binding of a concentration range of human and mouse antibodies (Figures only depict results for each primary anti-CD20 mAb at 30 μg/mL). Different numbers of maximum sABC were obtained for each specific cell line, correlated to the CD20 expression.

Secondly, we compared the newly developed human IgG calibrator assay to the mouse IgG calibrator assay by using variants of the CD20 mAb 7D8 with different backbones (human IgG1, mouse IgG1 and mouse IgG2a). We observed for the B-cell lymphoma cell lines Daudi (Figure 2B), Raji (S1), Ramos (S2) and the chronic B-cell leukaemia cell line MEC-1 (Figure 2C) that the mouse and human calibrator assays gave maximum sABC values of similar magnitude with mouse and human 7D8 antibody irrespective of IgG isotype. In contrast, the sABC obtained for mouse B9E9 was consistently lower than that for the other CD20 mAbs. This was also reported by Winiarska *et al.*[28] and is thought to be relevant for a type II CD20 mAb, although B9E9 has not been fully established as a type II mAb.

Similar results were obtained for B lymphocytes in WB (Figure 2D). For detection of B-lymphocytes in WB, we demonstrated that the value of the sABC obtained was not affected by the lysis procedure used (S3), the use of EDTA- or heparin- based anticoagulant (S4), or by extracellular matrix present. Daudi cells and Raji cells showed similar sABC before and after spiking into whole blood with both the human and mouse calibrator assays (respectively Figure 2E, huIgG1-7D8 and Figure 2F muIgG1-7D8 thus also excluded possible interference of membrane bound immunoglobulin (i.e. the B-cell receptor) in quantification of antigen-bound human antibodies. RTX and OFA showed similar numbers of sABC both on cell lines as well as healthy donor B lymphocytes tested (Figure 2B-D).

CD20 occupancy

Next, we used the human calibrator assay for determining target occupancy by the CD20 antibodies on B lymphocytes in WB. To establish the baseline level of antigen expression, we incorporated an acidic wash step to assess background and total mAb, even after the target antigen was occupied (e.g. during therapeutic treatment). Indeed, we were able to remove bound RTX and OFA quantitatively by acid stripping as reprobing of these samples with buffer led to a background similar to initial background determined before stripping (Figure 3A third black bar and first open bar). Similarly, the acid wash procedure did not influence the amount of available receptors for quantification of antigen as saturating amounts of primary antibody led to similar sABC levels as before stripping (Figure 3A and 3B).

We then set out to determine target occupancy in whole blood. Figure 3C and 3D show the results for 2 representative donors tested for occupancy with OFA. Bound OFA (in ABC; closed circle; from a serial dilution of OFA) and total OFA (maximum ABC; closed squares; by adding an additional saturating amount of OFA to a duplicate sample) measured with the human calibrator assay are depicted. Stripping and reprobing with a saturating amount of OFA (total OFA after stripping, Figure 3C and 3D open squares) or buffer (background, Figure 3C and 3D, closed triangles) mark the window of occupation.

Some donor variation exists, however this does not affect the occupancy determinations as is observed in Figure 3E. In these figures, the occupancy for both OFA and RTX is compared.

From the plotted occupancy of RTX and OFA against the concentration of the mAb used we deducted the EC_{50} for both antibodies for CD20 expressed on human B-cells (1.02 ± 0.37 µg/mL and 0.66 ± 0.16 µg/mL, respectively).

Dissociation and internalization measurements

In a final set of experiments, the apparent dissociation rates of OFA and RTX were determined by studying bound CD20 mAbs over time in the presence of an excess amount of mouse CD20 mAb muIgG1-7D8 to prevent OFA or RTX re-binding. The binding half-life ($t_{1/2}$) of RTX on B-lymphocytes in WB was 40 min (Figure 4A) while

FIGURE 3 Both the background and maximal sABC detection can be assessed by incorporating an acidic wash procedure in the quantification process at any time during a clinical trial.
Here bound CD20 antibody can be eluted without affecting CD20 re-detection on B-lymphocytes from WB. CD20 expression or detection was not affected as shown for detection with RTX (**A**) or OFA (**B**). Figures are summary of 4 independent assays and error bar represents SD.
Using the procedure described under material and methods section calculations the occupancy of OFA and RTX on B-lymphocytes from WB is determined. OFA occupancy of 2 representative donors is shown (**C** and **D**). In step 1 a serial dilution of OFA was used. In step 2 either buffer was added (Bound OFA, closed circles), a saturating concentration of OFA (Total OFA, closed squares) or acidic wash procedure followed by buffer (background, closed triangles) or a saturating concentration of OFA (Total OFA, after strip, open squares). Using total antibody (ABC) and bound antibody (ABC) data obtained using RTX or OFA in WB, the occupancy was determined and plotted in panel **E**.

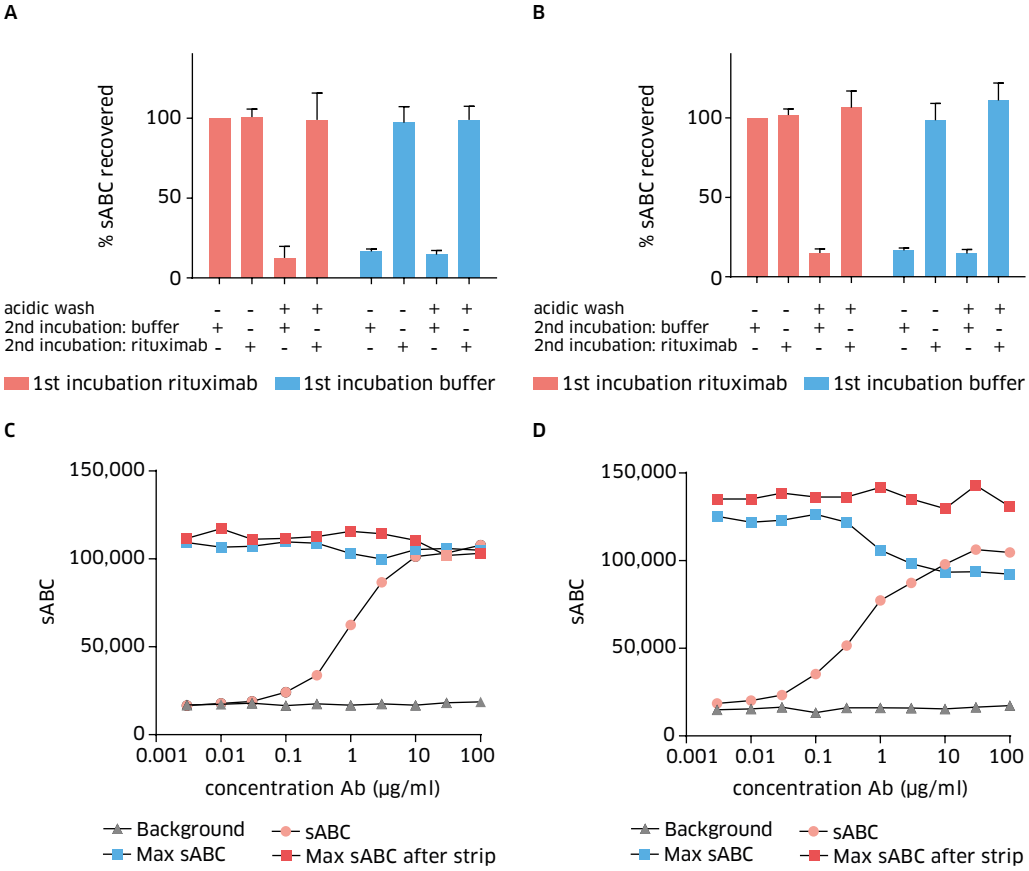
A
% sABC recovered
100
50
0
acidic wash - - + + - - + +
2nd incubation: buffer + - + - + - + -
2nd incubation: rituximab - + - + - + - +
1st incubation rituximab
1st incubation buffer
B
% sABC recovered
100
50
0
acidic wash - - + + - - + +
2nd incubation: buffer + - + - + - + -
2nd incubation: rituximab - + - + - + - +
1st incubation rituximab
1st incubation buffer
C
sABC
150,000
100,000
50,000
0
0.001 0.01 0.1 1 10 100
concentration Ab (µg/ml)
Background
Max sABC
sABC
Max sABC after strip
D
sABC
150,000
100,000
50,000
0
0.001 0.01 0.1 1 10 100
concentration Ab (µg/ml)
Background
Max sABC
sABC
Max sABC after strip
E
% occupancy
100
50
0
0.001 0.01 0.1 1 10 100
concentration Ab (µg/ml)
OFA (n=5)
RTX (n=4)

the $t_{1/2}$ for OFA was approximately 6 times longer (248 min) (Figure 4B). Combining the human calibrator assay with the mouse calibrator assay in this experiment, allowed us to obtain information on antigen kinetics. Thus we observed that CD20 antigen, from which RTX was dissociated, was quickly re-occupied by muIgG1-7D8. However, at later time points, a decrease of mouse antibody binding was seen despite the excess of muIgG1-7D8 added. The sum of human antibody and mouse antibody occupancy can be used to determine the total percentage of available binding sites. Using this analysis, we observed that incubation with RTX led to a ~60% decrease in CD20 binding sites over a 4-hour timeframe (Figure 4C). For OFA we observed a relatively sharp drop of % occupancy during the first 15 minutes after which approximately 20% OFA dissociated in the next 4 hours in line with a similar increase in muIgG1-7D8 binding (Figure 4D). The initial drop in OFA sABC is not accompanied by an increase in binding sites for the muIgG1-7D8 antibody which indicates that it likely is not the result of OFA dissociation. The effect may therefore be due to a reduced detection of OFA molecules by the secondary antibody (e.g. steric hindrance) as a result of CD20 antigen clustering which is characteristic following binding of type I CD20 mAb or CD20 internalization.

The sum of human and mouse antibody occupancy in the OFA experiment shows that the number of CD20 binding sites after this first initial drop remains relatively constant. These data suggest that loss of CD20 antigen binding sites occur more slowly for OFA than for RTX.

DISCUSSION

Although CD20 directed immunotherapy initially depletes all peripheral B-cells inevitably malignant lymphocytes repopulate the periphery. This, together with the fact that current dosing regimens might not optimal [29] warrants novel approaches to monitor therapeutic efficacy. Monitoring CD20 expression and occupancy by therapeutic antibody on malignant B-cells in the clinic is critical for the development of personalized medicine approaches. Thus the probability of clinical efficacy can be maximized by taking treatment-associated factors that influence target surface expression or accessibility to the therapeutic antibody into account [11, 12, 16, 28]. One of these factors is CD20 occupancy, which, in part, determines the effector mechanism employed by the antibody. Generally, it is observed that ADCC is triggered at lower occupancy than CDC as for example has been studied in detail for CD20 and EGFR antibodies [1, 4, 30]. These dose-effect relationships are both antigen- and epitope-dependent. Thus, type I CD20 antibodies such as OFA and RTX are particularly efficient in their ability to induce CDC, yet maximal ADCC is achieved at lower occupancy than maximal CDC [2, 4]. The impact of epitope is shown by the observation that RTX requires a higher occupancy level than OFA to achieve efficient CDC [1-3, 31]. Decreasing surface expression may thus result in a level of occupancy where antibodies can elicit both CDC and ADCC to an occupancy where only ADCC can be elicited and then to a point where both are inactive. Thus precise quantification of target cell occupancy of a specific therapeutic antibody might be

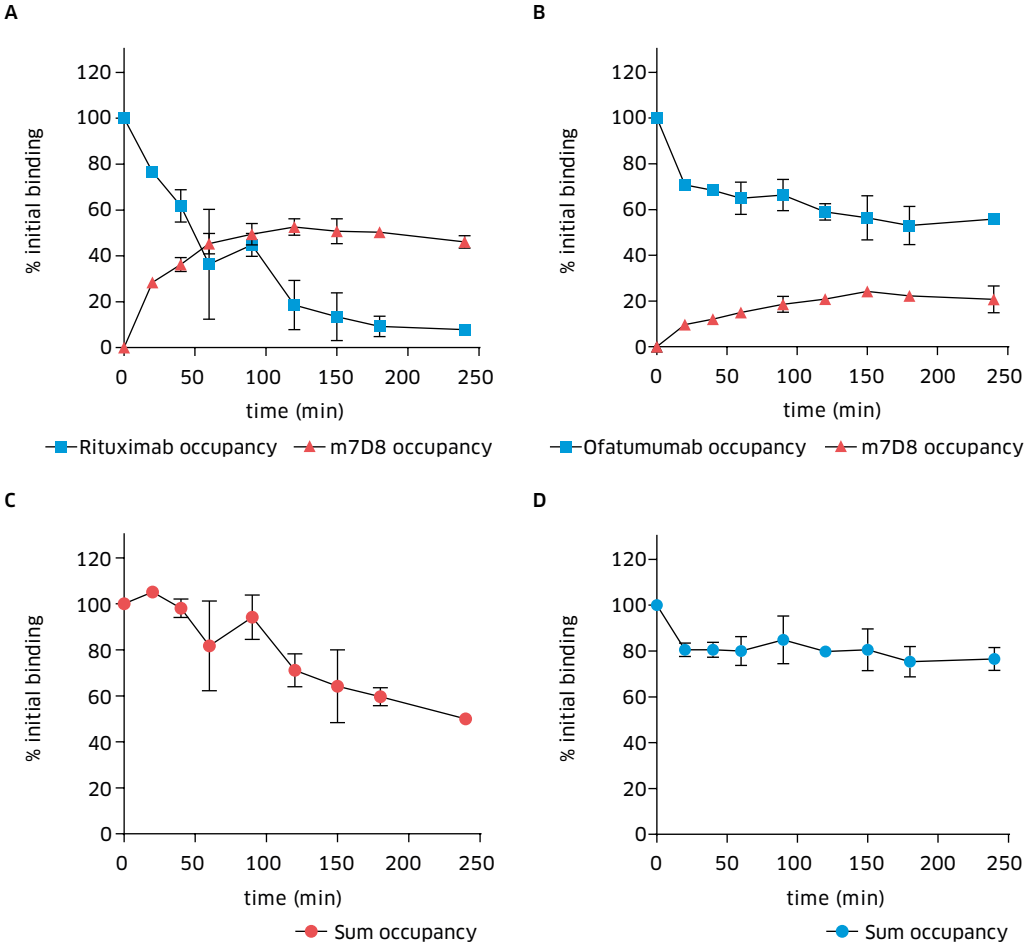

FIGURE 4 **Occupancy of RTX and OFA.**

The Occupancy of RTX and OFA in the presence of muIgG1-7D8 competitor was determined on B-lymphocytes from WB (respectively Fig 4A and 4B) over the time. The sum of RTX and muIgG1-7D8 mAbs occupancies was calculated allowing the determination of total occupancy of CD20 (Fig 4C). Similar curve with OFA is depicted (Fig 4D). Results shown are means of 2 individual experiments with error bars indicating SD.

Results show that combining both calibrator assays results in the Koff measurements of human antibody and antigen internalization with mouse antibody.

The time point where half of the initial amount of ofatumumab is detected (detection half-life) as being bound to Daudi cells is 248 min, whereas for rituximab already after 40 min the signal was reduced to 50% (data not shown).

MuIgG1-7D8 binding was detected with the mouse IgG calibrator assay. Initially muIgG1-7D8 replaces dissociated RTX resulting in an increase of muIgG1-7D8 in time. However after all bound rituximab has been replaced by muIgG1-7D8, we observed a decrease in detection of muIgG1-7D8 reflecting the internalization of the antigen. In the presence of OFA only very limited amounts of muIgG1-7D8 could be detected indicating that the measured reduction in binding signal reflects the internalization of antigen-antibody complexes rather than the dissociation of OFA.

correlated with mechanism of action knowledge to predict and monitor therapeutic efficacy.

Here, we describe a new quantitative flow cytometry assay which is primarily intended for quantification of chimeric, humanized or human therapeutic antibodies bound to the surface of (malignant) cells (Figure **1**). In addition, the assay can be used to detect antigenic modulation by such therapeutic agents as well as for studying the kinetics of antibody binding.

In this study we have shown that the human calibrator assay is as accurate in determining surface antigen in sABC as the well validated mouse calibrator assay. Moreover, antibody characteristics were comparable to previous observations. First, saturating levels of antibody on WB samples from healthy donors were consistent with previous observations published by Teeling [31].

Second, the antibody binding property such as EC50 of RTX observed here (6.8 nM) is similar to previous reported data by Reff (5.2 nM) [32] and Li (4.9 nM) [33]. The limited variation between EC50 values is potentially due to cell lines used.

Third, the half-life (t½) (40 min for RTX and 248 min for OFA) correlated with Li [33] and Teeling [31] (80 min for RTX and 70% OFA still occupied up to at least 3 hrs).

Fourth, the decrease of available binding sites for RTX we observed in this study (after 4 hours only 60% of the binding sites as measured at t=0 remained) was similar to the recently described internalization rate of RTX [11]. Interestingly, after an initial decrease of 20% of OFA binding sites detected after 15 min, we did not see a further decrease of OFA binding sites presumably because the OFA-CD20 complex does not internalize, although this will have to be investigated further. The differences in internalization rate between OFA and RTX might partially explain the differences found in CDC induction by these therapeutic agents.

It is important to note that it is well established that although all CD20 mAb compete for binding, they do not all detect the same number of CD20 binding sites. Thus, quantification of CD20 using type I and type II anti-CD20 mAbs gives different results, with type II mAb consistently showing about half the number of sABC compared to type I mAb [31,34]. These differences may be due to epitope and different orientation of binding [3,35]. Thus, the quantification of total and bound CD20 in terms of sABC is directly dependent on the reporter mAb that is used.

All in all, this assay provides a more correct approach to calculate the off-rate for therapeutic antibodies, as this assay may be used to adjust for total CD20 at the surface of the cell membrane, and thus for internalization. The detection half-life thus reflects the total amount of anti-CD20 molecules remaining on the surface and is therefore the result of both anti-CD20 dissociation and CD20 internalization.

Taken together this new assay is able to quantify chimeric, humanized or human antibodies bound to their target cell surface and can provide valuable information on such antibodies both in a research setting as in a clinical setting.

The human IgG calibrator can be applied to study the kinetics of therapeutic antibody binding in patient samples such as whole

blood. This method, potentially together with the acid stripping procedure, results in the ability to measure antigen binding of therapeutic antibodies in correlation to antigen surface expression. Thus, it allows evaluating, monitoring and adapting therapeutic regimens on an individual patient's basis and thereby adds to the development of personalized medicine.

Acknowledgements
We thank S.R. Ruuls and W.K. Bleeker for critical review of the manuscript.

Conflict of interest
P.J. Engelberts: Employment Genmab. F.J. Beurskens: Employment Genmab. P.W.H.I. Parren: Employment Genmab; owns warrant in Genmab as employee benefit. C. Badoil: Employment BioCytex. D. Boulay-Moine: Employment BioCytex. K. Grivel: Employment BioCytex. M. Moulard: Employment BioCytex.

REFERENCES

1 van Meerten, T., et al., *HuMab-7D8, a monoclonal antibody directed against the membrane-proximal small loop epitope of CD20 can effectively eliminate CD20 low expressing tumor cells that resist rituximab-mediated lysis.* Haematologica, 2010. **95**(12): p. 2063-71.

2 van Meerten, T., et al., *Complement-induced cell death by rituximab depends on CD20 expression level and acts complementary to antibody-dependent cellular cytotoxicity.* Clin Cancer Res, 2006. **12**(13): p. 4027-35.

3 Teeling, J.L., et al., *The biological activity of human CD20 monoclonal antibodies is linked to unique epitopes on CD20.* J Immunol, 2006. **177**(1): p. 362-71.

4 Bleeker, W.K., et al., *Estimation of dose requirements for sustained in vivo activity of a therapeutic human anti-CD20 antibody.* Br J Haematol, 2008. **140**(3): p. 303-12.

5 D'Arena, G., et al., *Quantitative flow cytometry for the differential diagnosis of leukemic B-cell chronic lymphoproliferative disorders.* Am J Hematol, 2000. **64**(4): p. 275-81.

6 Huh, Y.O., et al., *Higher levels of surface CD20 expression on circulating lymphocytes compared with bone marrow and lymph nodes in B-cell chronic lymphocytic leukemia.* Am J Clin Pathol, 2001. **116**(3): p. 437-43.

7 Olejniczak, S.H., et al., *A quantitative exploration of surface antigen expression in common B-cell malignancies using flow cytometry.* Immunol Invest, 2006. **35**(1): p. 93-114.

8 Hulkkonen, J., et al., *Surface antigen expression in chronic lymphocytic leukemia: clustering analysis, interrelationships and effects of chromosomal abnormalities.* Leukemia, 2002. **16**(2): p. 178-85.

9 Tam, C.S., et al., *Chronic lymphocytic leukaemia CD20 expression is dependent on the genetic subtype: a study of quantitative flow cytometry and fluorescent in-situ hybridization in 510 patients.* Br J Haematol, 2008. **141**(1): p. 36-40.

10 Ginaldi, L., et al., *Levels of expression of CD19 and CD20 in chronic B cell leukaemias.* J Clin Pathol, 1998. **51**(5): p. 364-9.

11 Beers, S.A., et al., *Antigenic modulation limits the efficacy of anti-CD20 antibodies: implications for antibody selection.* Blood. **115**(25): p. 5191-201.

12 Hiraga, J., et al., *Down-regulation of CD20 expression in B-cell lymphoma cells after treatment with rituximab-containing combination chemotherapies: its prevalence and clinical significance.* Blood, 2009. **113**(20): p. 4885-93.

13 Beum, P.V., et al., *The shaving reaction: rituximab/CD20 complexes are removed from mantle cell lymphoma and chronic lymphocytic leukemia cells by THP-1 monocytes.* J Immunol, 2006. **176**(4): p. 2600-9.

14 Beum, P.V., M.A. Lindorfer, and R.P. Taylor, *Within peripheral blood mononuclear cells, antibody-dependent cellular cytotoxicity of rituximab-opsonized Daudi cells is promoted by NK cells and inhibited by monocytes due to shaving.* J Immunol, 2008. **181**(4): p. 2916-24.

15 Williams, M.E., et al., *Thrice-weekly low-dose rituximab decreases CD20 loss via shaving and promotes enhanced targeting in chronic lymphocytic leukemia.* J Immunol, 2006. **177**(10): p. 7435-43.

16 Czuczman, M.S., et al., *Acquirement of rituximab resistance in lymphoma cell lines is associated with both global CD20 gene and protein down-regulation regulated at the pretranscriptional and posttranscriptional levels.* Clin Cancer Res, 2008. **14**(5): p. 1561-70.

17 Bil, J., et al., *Bortezomib modulates surface CD20 in B-cell malignancies and affects rituximab-mediated complement-dependent cytotoxicity.* Blood, 2010. **115**(18): p. 3745-55.

18 Boross, P., et al., *Both activating and inhibitory Fc gamma receptors mediate rituximab-induced trogocytosis of CD20 in mice.* Immunol Lett, 2012. **143**(1): p. 44-52.

19 Schwartz, A., et al., *Standardizing flow cytometry: construction of a standardized fluorescence calibration plot using matching spectral calibrators.* Cytometry, 1996. **26**(1): p. 22-31.

20 Henderson, L.O., et al., *Terminology and nomenclature for standardization in quantitative fluorescence cytometry.* Cytometry, 1998. **33**(2): p. 97-105.

21 Serke, S., A. van Lessen, and D. Huhn, *Quantitative fluorescence flow cytometry: a comparison of the three techniques for direct and indirect immunofluorescence.* Cytometry, 1998. **33**(2): p. 179-87.

22 Marti, G.E., A. Gaigalas, and R.F. Vogt, Jr., *Recent developments in quantitative fluorescence calibration for analyzing cells and microarrays.* Cytometry, 2000. **42**(5): p. 263.

23 Jasper, G.A., et al., *Variables affecting the quantitation of CD22 in neoplastic B cells.* Cytometry B Clin Cytom, 2011. **80**(2): p. 83-90.

24 Davis, K.A., et al., *Determination of CD4 antigen density on cells: role of antibody valency, avidity, clones, and conjugation.* Cytometry, 1998. **33**(2): p. 197-205.

25 Zenger, V.E., et al., *Quantitative flow cytometry: inter-laboratory variation.* Cytometry, 1998. **33**(2): p. 138-45.

26 Leget, G.A. and M.S. Czuczman, *Use of rituximab, the new FDA-approved antibody.* Curr Opin Oncol, 1998. **10**(6): p. 548-51.

27 Wierda, W.G., et al., *Ofatumumab as single-agent CD20 immunotherapy in fludarabine-refractory chronic lymphocytic leukemia.* J Clin Oncol, 2010. **28**(10): p. 1749-55.

28 Winiarska, M., et al., *Statins impair antitumor effects of rituximab by inducing conformational changes of CD20.* PLoS Med, 2008. **5**(3): p. e64.

29 Beurskens, F.J., et al., *Exhaustion of cytotoxic effector systems may limit monoclonal antibody-based immunotherapy in cancer patients.* J Immunol, 2012. **188**(7): p. 3532-41.

30 Lammerts van Bueren, J.J., et al., *Effect of target dynamics on pharmacokinetics of a novel therapeutic antibody against the epidermal growth factor receptor: implications for the mechanisms of action.* Cancer Res, 2006. **66**(15): p. 7630-8.

31 Teeling, J.L., et al., *Characterization of new human CD20 monoclonal antibodies with potent cytolytic activity against non-Hodgkin lymphomas.* Blood, 2004. **104**(6): p. 1793-800.

32 Reff, M.E., et al., *Depletion of B cells in vivo by a chimeric mouse human monoclonal antibody to CD20.* Blood, 1994. **83**(2): p. 435-45.

33 Li, B., et al., *Characterization of a rituximab variant with potent antitumor activity against rituximab-resistant B-cell lymphoma.* Blood, 2009. **114**(24): p. 5007-15.

34 Mossner, E., et al., *Increasing the efficacy of CD20 antibody therapy through the engineering of a new type II anti-CD20 antibody with enhanced direct and immune effector cell-mediated B-cell cytotoxicity.* Blood, 2010. **115**(22): p. 4393-402.

35 Niederfellner, G., et al., *Epitope characterization and crystal structure of GA101 provide insights into the molecular basis for type I/II distinction of CD20 antibodies.* Blood, 2011. **118**(2): p. 358-67.

SUPPLEMENTARY FIGURES

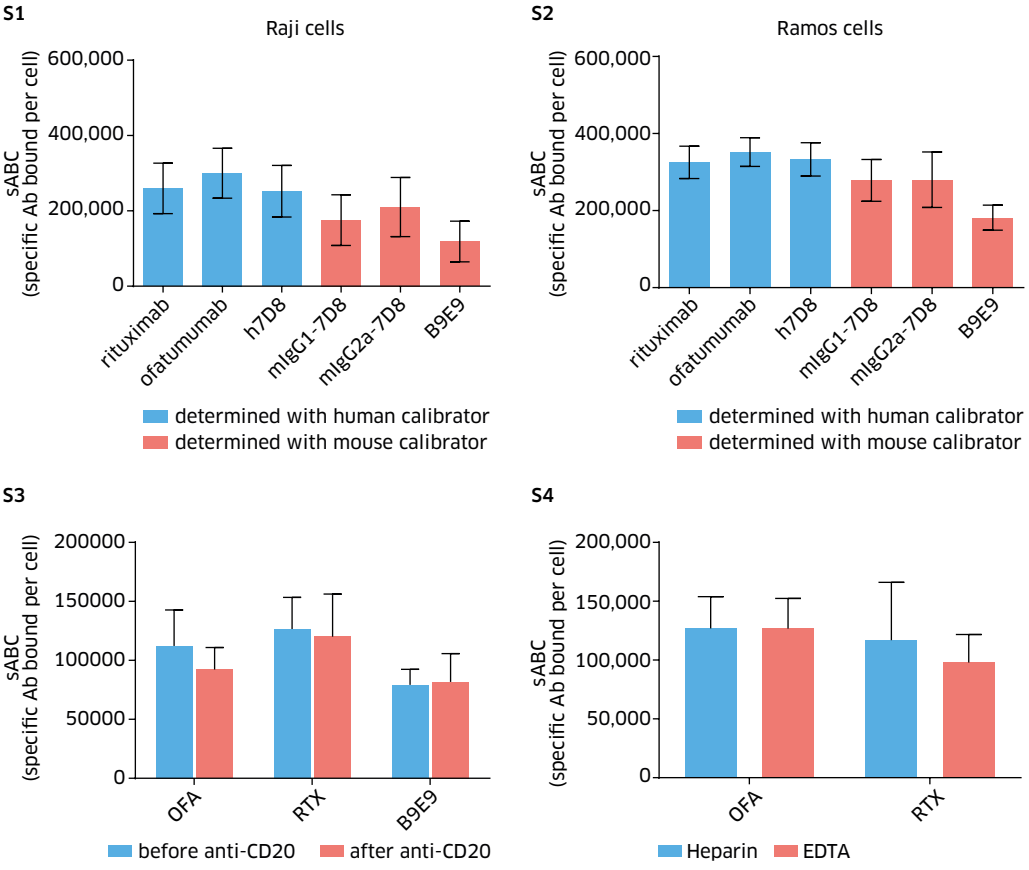

SUPPLEMENTARY FIGURE 1 **Control experiments.**